Sensors and Actuators B 212 (2015) 481–486

Contents lists available at ScienceDirect

Sensors and Actuators B: Chemical

journal homepage: www.elsevier.com/locate/snb

Gold nanoparticle-based colorimetric detection of mercury ion via coordination chemistry

Jianjun Du*, Zhenkuan Wang, Jiangli Fan, Xiaojun Peng

State Key Laboratory of Fine Chemicals, Dalian University of Technology, 2 Linggong Road, Dalian 116024, PR China

ARTICLE INFO

Article history:
Received 15 November 2014
Received in revised form 27 January 2015
Accepted 27 January 2015
Available online 16 February 2015

Keywords:
Colorimetric assay
Gold nanoparticle
Coordination chemistry
Thymine derivative
Mercury ion

ABSTRACT

A simple, fast, and convenient colorimetric detection of Hg^{2+} in aqueous media was presented based on the selective binding capability of thymine derivative (**N-T**) toward Hg^{2+}. **N-T** decorated AuNPs solution was stable in red color, while the presence of Hg^{2+} induces significant aggregation of AuNPs along with red-to-blue color changes. Therefore, Hg^{2+} content in real water samples can be qualitatively detected by our naked eyes; meanwhile, good linear relationship of Hg^{2+} along with $A_{650\ nm/520\ nm}$ values could be obtained for its quantitative determination. Furthermore, our system shows excellent selectivity to mercury ions against any other tested metal ions and anions, and good sensitivity with LOD of 0.8 nM in real water samples.

1. Introduction

Mercury is one of the most useful metal elements in paints, mining, pesticides, ammunition factory and so on [1,2], which meanwhile lead to the widespread mercuric contaminations [3]. Increasing concerns over mercury exposure and its deleterious effects on public health and environment safety promote developing fast, specific, low-cost, and efficient tools as well as tactics for mercury ion detection [4]. Compared with complicated instrument-based methods, gold nanoparticles (AuNPs)-based colorimetric assay [5–8] has drawn increasing attention due to its greater absorption extinction coefficient, tunable surface plasmon resonances (SPRs) and naked eye-distinguishable readouts, which make it one of the most suitable strategies for practical applications [9,10]. Therefore, by adjustable external stimulations [11–13], AuNPs-based assay is applied in the study of protein [14–16], enzyme [17–19], DNA [20,21], biomolecules [22,23], and ions [24–27], showing excellent sensitivity, accuracy, and fast colorimetric changes [28,29]. Recently, dsDNA [30–33] (with thymine–thymine mismatch) and ssDNA [34,35] (with plenty of thymine) have been designed and synthesized for colorimetric detection of Hg^{2+} based on the specific binding capability of thymine to Hg^{2+} [36,37]. Then, to avoid the synthesis of DNA and accurate control in following detection (such as the melting temperature of dsDNA), functional molecules have been presented based on the coordination chemistry and mild redox reaction [38–51]. Nevertheless, some systems, such as some acid-AuNPs systems, suffer from interference of other metal ions (such as Pb^{2+} and Cd^{2+}), wherein mask agents have to be introduced, while for redox-based system, Ag^{+} is clearly one of the biggest threats. Therefore, the main challenge is to develop a selective, sensitive, and stable system that can avoid these consequences.

In this context, with the above motivations, intense endeavor has been dedicated to presenting a fast, sensitive, and stable AuNPs system for Hg^{2+} sensing especially with good selectivity and anti-interference capability. Thymine has been proved to be one of the best ligands for selectively catching Hg^{2+} [52–54], though poor solubility in neutral aqueous media could affect its sensing capability. In this work, we thereby introduce a hydrophilic group to endow thymine better performance for Hg^{2+} detection in aqueous samples. As a proof-of-concept, we synthesized and applied a thymine derivative modified with quaternary ammonium salt (**N-T**, as shown in Scheme 1), which was introduced not only to increase the water solubility but also to act as an anchor by electrostatic effect when functionalized on gold surface. The **N-T** was synthesized according to the published literatures [55,56]. Scheme 1 illustrates the working principle of our colorimetric system. The **N-T** decorated AuNPs (13 nm) solution displays red color with absorption peak at about 520 nm, while the presence of Hg^{2+} induces fast aggregation of AuNPs along with significant

* Corresponding author. Tel.: +86 41184986327.
E-mail address: dujj@dlut.edu.cn (J. Du).

http://dx.doi.org/10.1016/j.snb.2015.01.110
0925-4005/

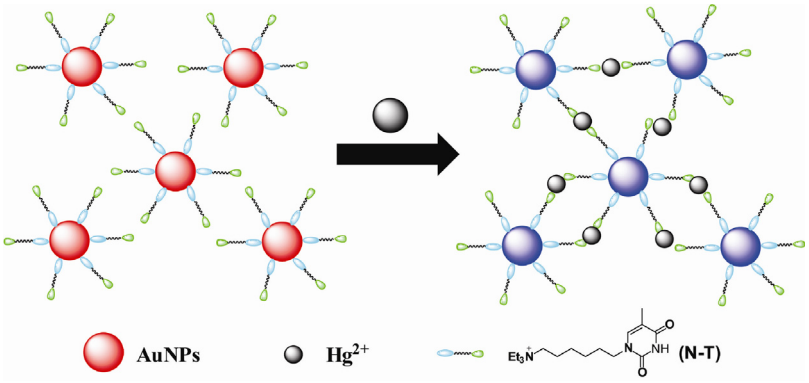

Scheme 1. Schematic illustration of **N-T**/AuNPs-based colorimetric detection of Hg^{2+}.

red-to-blue color change. Thanks to respective functions of thymine and quaternary ammonium, this system realizes fast, sensitive, and selective detection of Hg^{2+} in aqueous media without masking agent. And the limit of detection (LOD) reached as low as 0.8 nM in real water systems, which endows our system's capability of distinguishing safe water from Hg^{2+} polluted samples.

2. Experimental

2.1. Chemicals

Gold(III) chloride trihydrate (99.9+%) was purchased from Sigma–Aldrich. The solutions of anions and metal ions were prepared from NaCl, $MgCl_2{\cdot}6H_2O$, $CoCl_2{\cdot}6H_2O$, $ZnCl_2$, $CdCl_2$, $CaCl_2$, $BaCl_2$, $CuCl_2{\cdot}2H_2O$, $PbCl_2$, $NiCl_2$, $CrCl_3$, $MnSO_4$, KBr, $AgNO_3$, $HgCl_2$, $FeCl_3{\cdot}6H_2O$, NaSCN, Na_2SO_4, $NaClO_4{\cdot}H_2O$, KI, NaOAc, KBr, KCl, $Na_2P_2O_7$, $K_2HPO_4{\cdot}3H_2O$, Na_3PO_4, $NaNO_3$, $NaNO_2$, and Na_2CO_3, by separately dissolving each metal ion in distilled water. All other chemicals were supplied by Aladdin Reagent Company and Energy Chemical Reagent Company, and were used as received.

2.2. Instruments

^{1}H NMR spectra were recorded on a VARIAN INOVA-400 spectrometer with chemical shifts (δ) reported as ppm (in $CDCl_3$, TMS as the internal standard). Mass spectrometry data were obtained with an HP1100LC/MSD mass spectrometer and an LC/Q-TOF MS spectrometer. AuNPs were characterized by transmission electron microscopy (TEM, T20) at 200 kV. Absorption spectra were measured on a Lambda 35 UV/Vis spectrophotometer (Perkin Elmer). All pH measurements were made with a Model PHS-3C meter. The zeta potentials of AuNPs before and after modification by **N-T** were measured by ZETASIZER nano series Nano-ZS90.

2.3. Synthetic procedures

The synthesis of **N-T** followed the general route as shown in Fig. S1.

Synthesis of ***1***: Potassium carbonate (3.03 g, 3.00 mmol) was added into a suspension of thymine (0.93 g, 1.00 mmol) in dry DMF (20 mL), and the mixture was heated at 40 °C for 1 h. After the mixture was cooled to room temperature, 1,6-dibromohexane (5.41 g, 3.00 mmol) was added, and the resulting mixture was heated at 40 °C for 3 h whereupon it was evaporated. The crude was treated with CH_2Cl_2 (150 mL) and filtered. The filtrate was purified by silica gel column chromatography (EtOAc/hexane) to afford **1** (704 mg, 33.4%). ^{1}H NMR (400 MHz, $CDCl_3$), δ: 8.93 (s, 1H), 6.98 (s, 1H), 3.70 (t, J = 8 Hz, 2H), 3.41 (t, J = 8 Hz, 2H), 1.98 (t, 3H), 1.87 (m, 2H), 1.70 (m, 2H), 1.50 (m, 2H), 1.36 (m, 2H); MS: ($C_{11}H_{17}BrN_2O_2$ $[M+H]^+$) m/z 289.11.

Synthesis of **N-T**: **1** (156 mg, 0.57 mmol) and a spot of KI in dry DMF (5 mL) were added into a flask (50 ml) in ice-bar. The triethylamine (818 mg, 8.1 mmol) was then added. The ice bath was then removed, and the solution was stirred at 80 °C for 2 h whereupon it was evaporated. The crude was purified by neutral alumina column chromatography (CH_2Cl_2/CH_3OH) to afford **N-T** (85 mg, 50.3%). ^{1}H NMR (400 MHz, $CDCl_3$), δ: 8.63 (s, 1H), 7.36 (s, 1H), 3.76 (t, J = 8 Hz, 2H), 3.48 (q, J = 8 Hz, 6H), 3.39 (t, J = 8 Hz, 2H), 1.95 (s, 3H), 1.78 (m, 4H), 1.50 (m, 4H), 1.40 (t, J = 8 Hz, 9H); TOF MS: m/z calcd for $C_{17}H_{32}N_3O_2^+$ $[M]^+$: 310.2489, found: 310.2496.

Synthesis 13 nm AuNPs: AuNPs (13 nm) was prepared by sodium citrate reduction of a $HAuCl_4$ solution as described in the literature [57].

2.4. Fabrication of *N-T*/AuNPs system

The AuNPs solution was centrifuged (10,000 rpm, 15 min) before the following modification. In order to stabilize the AuNPs system, Tween 20 was introduced as stabilizer, which can protect AuNPs from aggregation induced by interferents and the stimulus in the test environment. According to the control experiment, 1 ppm Tween 20 was proved optimal which was used in this work (Fig. S2).

And then quantitative **N-T** was added into Tween 20-protected AuNPs solution to simplify the fabrication of **N-T**/AuNPs system. When 5 μM **N-T** was added, the $A_{650\ nm/520\ nm}$ value reached to about 1.1 which exhibited best efficiency for mercury ion sensing (Fig. S3). Therefore, 5 μM **N-T** was the optimal concentration for the modification. After 10 min incubation, **N-T**/AuNPs solutions were ready for testing. The zeta potentials of −25.8 mV and −18.0 mV were obtained before and after functionalization of positive **N-T** on gold surface, which confirmed the surface charge changes upon **N-T** modification.

2.5. Pretreatment of real water samples

Both the tap water (collected from our lab) and natural drinking water (Nongfu spring) were selected for practical detection of Hg^{2+}. Standard solutions of varying Hg^{2+} concentrations (50–250 nM) were prepared from a concentrated stock solution with Hg^{2+} (0.5 mM) and were artificially added to the water samples. The pH value of these AuNP solutions was adjusted to 7.0. In the test, 500 μL **N-T**/AuNPs solution was added into 1000 μL water samples followed by UV–Vis spectra recording after 10 min incubation.

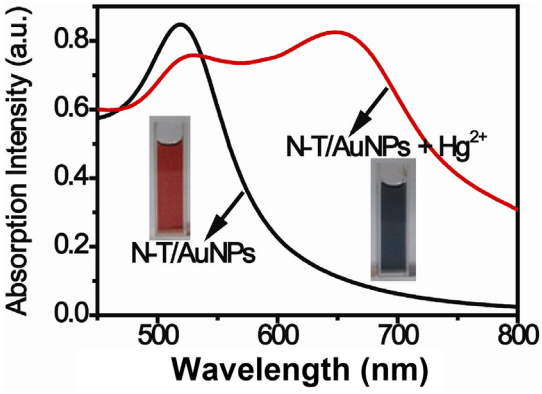

Fig. 1. Absorbance spectra and solution color of the **N-T**/AuNPs in the absence and presence of Hg^{2+} (1 μM).

3. Results and discussion

3.1. Hg^{2+} detection by ***N-T***/AuNPs and selectivity

N-T modified AuNPs solution (5.4 nM) was red in color with a SPR band at 520 nm, while a new board peak appeared obviously at around 650 nm along with red-to-blue color changes after Hg^{2+} was added into the system (Fig. 1). This can be ascribed to the thymine's bonding with Hg^{2+}, resulting in aggregation of AuNPs, which could also be proved by the UV–Vis spectroscopy changes of **N-T**/Hg^{2+} complexes compared with that of **N-T** and Hg^{2+}, respectively (Fig. S4).

Then, we evaluated the selective response of Hg^{2+} by adding various competitive metal ions and anions to the **N-T**/AuNPs solutions and monitoring both UV–Vis spectra and colorimetric changes at room temperature. As shown in Fig. 2a, among all the test metal ions (Na^+, K^+, Ca^{2+}, Mg^{2+}, Ag^+, Zn^{2+}, Pb^{2+}, Cu^{2+}, Co^{2+}, Ni^{2+}, Mn^{2+}, Fe^{3+}, Cr^{3+}, Cd^{2+}, and Hg^{2+}), only Hg^{2+} resulted in an obvious red-to-blue color change and increase of $A_{650\ nm/520\ nm}$ value. Further, we investigated the response of **N-T**/AuNPs system in the presence of various anions (Cl^-, Br^-, I^-, ClO_4^-, OAc^-, SCN^-, SO_4^{2-}, NO_3^-, NO_2^-, HCO_3^-, CO_3^{2-}, HPO_4^{2-}, $P_2O_7^{2-}$, and PO_4^{3-}). None of these anions could induce obvious aggregation of AuNPs as well as color change (Fig. 2b). These results proved the distinct capability of Hg^{2+} to aggregate **N-T**/AuNPs even in complicated ions-mixing environment.

3.2. Optimal condition of the assay

Predominantly, pH value is one of the most important factors that influenced most AuNPs system. Therefore, different pH values of AuNPs solution were also studied keeping other factors constant (such as the concentration of Hg^{2+} and AuNPs). As shown in Fig. 3a, the value of $A_{650\ nm/520\ nm}$ could reach to about 0.9 in neutral media (pH 7.0), much bigger than that of 0.38 and 0.41 in the acidic (pH 5.0) and alkaline (pH 9.0) solutions, respectively. In alkaline media, Hg^{2+} hydrolyzes easily, while in the acidic condition the system becomes unstable, wherein the $A_{650\ nm/520\ nm}$ value reached 0.26, much bigger than that of 0.14 in neutral media (Fig. 3a). Therefore, **N-T**/AuNPs system in pH 7.0 was optimal and used in the following tests.

Besides pH values, AuNPs concentration is another important factor which could affect the sensing efficiency of the AuNPs

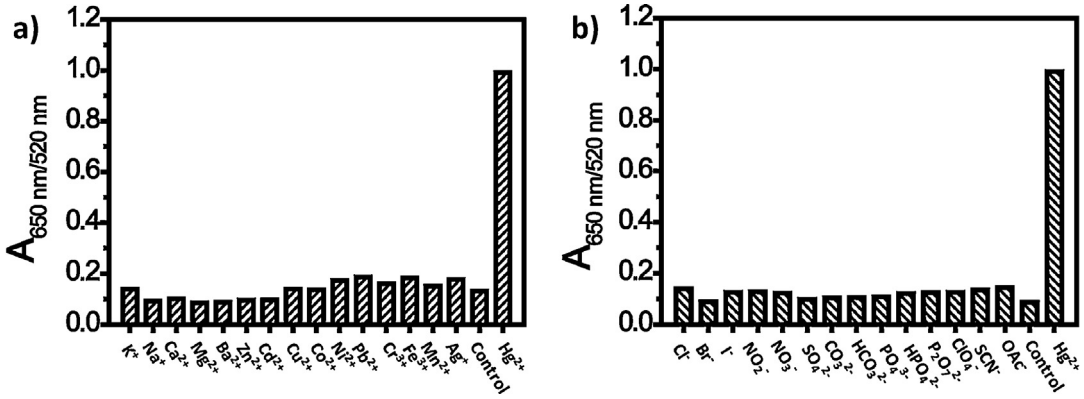

Fig. 2. Selectivity experiment of **N-T**/AuNPs system toward different interfere metal ions (a) (the Hg^{2+} concentration is 3 μM, Cr^{3+} is 20 μM, K^+, Na^+, Mg^{2+}, and Ca^{2+} are 500 μM, and others are 50 μM.) and anions (b) (the Hg^{2+} concentration is 3 μM and others are 50 μM).

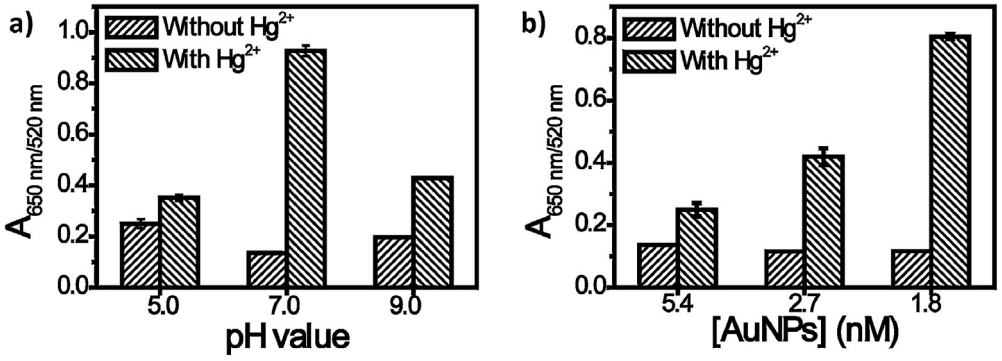

Fig. 3. (a) Effect of different pH values (a) and AuNPs concentrations (b) on the absorbance ratio ($A_{650\ nm/520\ nm}$) of the **N-T**/AuNPs in the absence and presence of Hg^{2+} (3.0 and 1.5 μM, respectively).

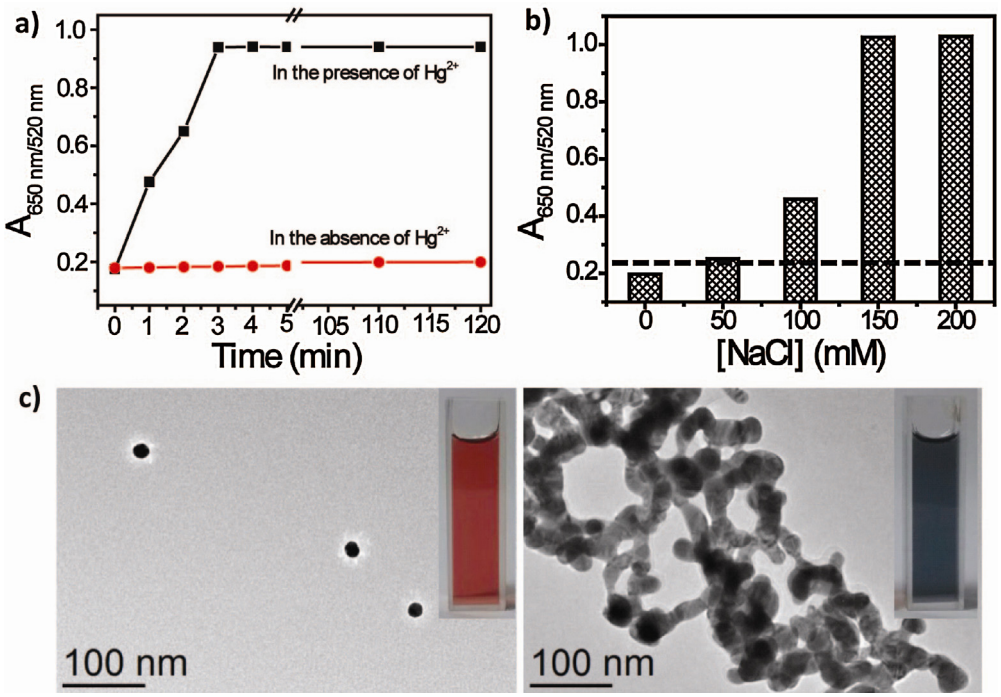

Fig. 4. (a) $A_{650\ nm/520\ nm}$ values of **N-T**/AuNPs system vs. time (min) in the absence and presence of Hg^{2+} (3 μM); (b) the $A_{650\ nm/520\ nm}$ values of **N-T**/AuNPs system in the absence and presence of different concentrations of NaCl (0, 50, 100, 150, and 200 mM); (c) SEM of **N-T**/AuNPs solutions in the absence (left) and presence (right) of Hg^{2+} (1.5 μM).

systems. When pH value was kept constant, AuNPs solution (5.4 nM) was diluted to 2.7 nM and 1.8 nM, respectively. The diluted samples exhibited better sensitivities showing increasing $A_{650\ nm/520\ nm}$ values (0.42 and 0.79, respectively), because the relative concentration of Hg^{2+} was increased actually compared to original AuNPs solution ($A_{650\ nm/520\ nm}$ value is about 0.26) (Fig. 3b). Therefore, AuNPs (1.8 nM, pH 7.0) were used in the following experiments.

In the optimal test condition, the **N-T**/AuNPs system was kept stable for at least 120 min because Tween 20 was introduced as

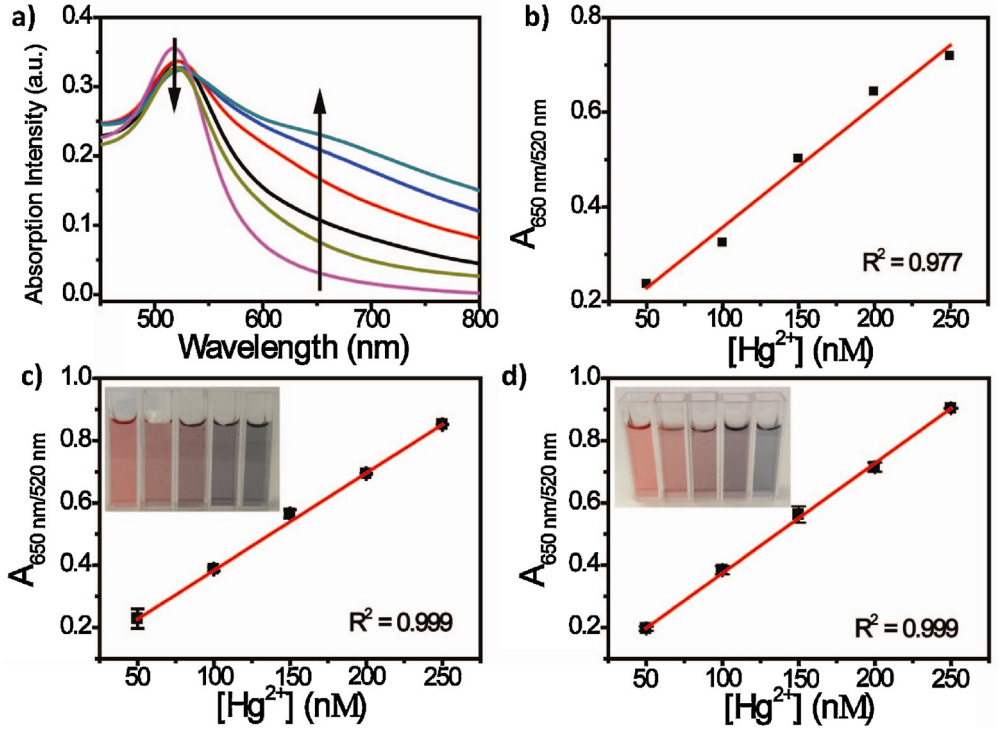

Fig. 5. (a) Absorbance spectra of the **N-T** (1.5 μM) modified AuNPs generated in the absence and presence of different concentrations of Hg^{2+}: (0, 50, 100, 150, 200, and 250 nM); (b) the linear relationship of the Hg^{2+} concentrations (50–250 nM) with $A_{650\ nm}/A_{520\ nm}$ and corresponding color changes in tap water (c) and natural drinking water (d) over the Hg^{2+} concentrations of 50–250 nM.

Table 1
Key characteristics of AuNP-based probes for colorimetric detection of Hg^{2+}.

Probe	LOD (nM)	Selectivity	Respond time (min)	Real sample	Ref.
Melamine-AuNPs by Chen et al.	50	Hg^{2+}	1	Lake water	[24]
Urine-AuNPs by Chen et al.	50	Hg^{2+}	2	Tap/lake water	[26]
DTET-AuNPs by Kim et al.	100	Hg^{2+} [a]	<10	–	[38]
MPA/AMP-AuNPs by Yu and Tseng et al.	500	Hg^{2+}	30	–	[39]
4-MB/AuNPs by Huang et al.	500	Hg^{2+}	30	River water	[40]
MTA-AuNPs by Wang and Jiang et al.	30	Hg^{2+}	–	–	[41]
Cysteine-AuNPs by Zhao, He, Zhang et al.	25	Hg^{2+} [a]	–	Drinking water	[42]
Tween 20-AuNPs by Tseng et al.	100	Hg^{2+}/Ag^{+}	5	Drinking/sea water	[43]
AA-AuNPs by Chen et al.	5	Hg^{2+}/Ag^{+}	3	Drinking/tap water	[44]
TA-AuNPs by Chai, Wang, and Qu et al.	10	Hg^{2+}	1	Lake water	[45]
Pyridine-AuNPs by Tian et al.	55	Hg^{2+}	10	Tap water	[46]
DPY-AuNPs by Zhong et al.	15	Hg^{2+}	30	Tap/Spring water	[47]
CA-AuNPs by Tian et al.	30	Hg^{2+}/melamine	10	Tap water	[48]
Tris/NTA-AuNPs by Chen and Gao et al.	7	Hg^{2+}	60	Lake water	[49]
1-Penicillamine/AuNPs by Huang et al.	25	Hg^{2+}	2	Tap water	[50]
Thymine-AuNPs by Chen et al.	2	Hg^{2+}	30	Tap water	[52]
Thymine-SH AuNPs by Chen et al.	2.8	Hg^{2+}	5	Tap water	[54]
N-T/AuNPs in this work	0.8	Hg^{2+}	1	Tap/drinking water	

[a] Using PDCA or EDTA as masking agents.

stabilizing agent in our system, wherein the $A_{650\ nm/520\ nm}$ values were kept below 0.2 all the time (Fig. 4a), while obvious red-to-blue color change could be observed within 1 min after addition of Hg^{2+}, due to the aggregation of AuNPs (Fig. 4a) and the $A_{650\ nm/520\ nm}$ value would become saturated within 4 min. The scanning electron microscope (SEM) images further demonstrated the well-dispersed (Fig. 4c, left) and following Hg^{2+}-induced aggregation of **N-T**/AuNPs (Fig. 4c, right). These results are consistent with the colorimetric change and corresponding UV–Vis spectra of AuNPs solution.

3.3. Sensitivity and analysis of Hg^{2+} in real samples

In order to evaluate the sensitivity of the assay, different concentrations of Hg^{2+} were tested. Quantitative performance toward Hg^{2+} was obtained by titrating Hg^{2+} into **N-T**/AuNPs solution. With increasing Hg^{2+} content gradually, the absorption intensity at 520 nm decreased a little with some red-shifts, and simultaneously the intensity at 650 nm increased dramatically until a board peak appeared (Fig. 5a). Over the range of 50–250 nM, the intensity ratio $A_{650\ nm/520\ nm}$ of **N-T**/AuNPs solution increased proportionally, which suggested good linear relationship with Hg^{2+} concentrations over the range of 50–250 nM (Fig. 5b). Depending on its excellent sensitivity, we tried to detect Hg^{2+} in real water samples in the following work.

More importantly, our colorimetric system could find potential application in the detection of Hg^{2+} not only in DI water but also in real water samples. The state of AuNPs could be affected distinctly by the salinity of samples, though Tween 20 was used as protective agent. Therefore, we studied the stability of our system with increasing addition of NaCl into the particle solution. The resistance against salt seems better along with the dilution of AuNPs solution (Fig. S5), and our system worked well when NaCl concentration is below 50 mM in the optimal condition (Fig. 4b). We chose tap water samples from our lab and drinking water from the "Nongfu spring". As shown in Fig. 5c and d, the $A_{650\ nm/520\ nm}$ value of **N-T**/AuNPs changed in the presence of difference Hg^{2+} (50–250 nM, artificial addition in water samples), wherein good linear relationship could be observed between $A_{650\ nm/520\ nm}$ values and Hg^{2+} concentrations ($R^2 = 0.999$) for both tap and natural drinking water samples, respectively. The limit of detection (LOD) reached 0.8 nM obtained from 3σ/slope [58]. Fig. 5 demonstrates the performance of the optimized sensor for quantitative detection of Hg^{2+} by our system, which proved the capability of **N-T**/AuNPs system in distinguishing between the safe and polluted levels of Hg^{2+} with naked eye-detectable color changes in real water samples. Compared with other examples in literatures, our system shows some better properties in LOD, selectivity, and response time as shown in Table 1.

4. Conclusion

In summary, we fabricated an **N-T**/AuNPs system, and its application as a colorimetric probe for Hg^{2+} detection based on thymine coordination chemistry. Besides the qualitative detection of mercury ion by colorimetric changes as well as lateral flow strip by naked eyes [59–61], quantitative determination and spatial mapping of mercury ion are also achieved by portable smart phones, which could be rather useful and convenient for sensing, tracking, and monitoring mercury contaminants [27,62]. With the development of the science and technology, for AuNPs based colorimetric detection of Hg^{2+}, its simplicity, fast, and naked eye-distinguishable colorimetric changes make it one of best promising detection methods for convenient detection and diagnostics.

Acknowledgments

This work was supported by the National Natural Science Foundation of China (21421005, 21406028, and 21136002), Doctoral Fund of Ministry of Education of China (20130041120014), The General Project of Liaoning Provincial Department of Education (L2013024), and the Fundamental Research Funds for the Central Universities (DUT14ZD214).

Appendix A. Supplementary data

Supplementary data associated with this article can be found, in the online version, at http://dx.doi.org/10.1016/j.snb.2015.01.110.

References

[1] E. Guallar, M.I. Sanz-Gallardo, P. van't Veer, P. Bode, A. Aro, J. Gomez-Aracena, J.D. Kark, R.A. Riemersma, J.M. Martin-Moreno, F.J. Kok, N. Engl. J. Med. 347 (2002) 1747–1754.
[2] A.S. Cabecinhas, S.C. Novais, S.C. Santos, A.C. Rodrigues, J.L. Pestana, A.M. Soares, M.F. Lemos, Chemosphere 119 (2014) 490–497.
[3] T.W. Clarkson, L. Magos, G.J. Myers, N. Engl. J. Med. 349 (2003) 1731–1737.
[4] P.B. Tchounwou, W.K. Ayensu, N. Ninashvili, D. Sutton, Environ. Toxicol. 18 (2003) 149–175.
[5] J.J. Du, L. Jiang, Q. Shao, X.G. Liu, R.S. Marks, J. Ma, X.D. Chen, Small 9 (2013) 1467–1481.
[6] D.B. Liu, Z. Wang, X.Y. Jiang, Nanoscale 3 (2011) 1421–1433.
[7] Y.W. Lin, C.C. Huang, H.T. Chang, Analyst 136 (2011) 863–871.
[8] M.R. Knecht, M. Sethi, Anal. Bioanal. Chem. 394 (2009) 33–46.

[9] Y.J. Huang, L. Wu, X.D. Chen, P. Bai, D.H. Kim, Chem. Mater. 25 (2013) 2470–2475.
[10] L. Jiang, C.J. Zou, Z.H. Zhang, Y.H. Sun, Y.Y. Jiang, W. Leow, B. Liedberg, S.Z. Li, X.D. Chen, Small 10 (2014) 609–616.
[11] Y.Y. Jiang, F.B. Meng, D.P. Qi, P.Q. Cai, Z.Y. Yin, F.W. Shao, H. Zhang, F. Boey, X.D. Chen, Small 9 (2013) 2260–2265.
[12] L. Jiang, Y.H. Sun, F.W. Huo, H. Zhang, L.D. Qin, S.Z. Li, X.D. Chen, Nanoscale 4 (2012) 66–75.
[13] X.G. Han, Y.D. Liu, Y.D. Yin, Nano Lett. 14 (2014) 2466–2470.
[14] H. Xu, J. Chen, J. Birrenkott, J.X. Zhao, S. Takalkar, K. Baryeh, G. Liu, Anal. Chem. 86 (2014) 7351–7359.
[15] C.C. Chang, C.Y. Chen, X.H. Zhao, T.H. Wu, S.C. Wei, C.W. Lin, Analyst 139 (2014) 3347–3351.
[16] X.H. Liu, Y. Wang, P. Chen, Y.S. Wang, J.L. Mang, D. Aili, B. Liedberg, Anal. Chem. 86 (2014) 2345–2352.
[17] L. Hou, Y. Tang, M. Xu, Z. Gao, D. Tang, Anal. Chem. 86 (2014) 8352–8358.
[18] Y.B. Fan, F.Y. Li, D.Y. Chen, Biomaterials 35 (2014) 7870–7880.
[19] Y. Xiao, F. Patolsky, E. Katz, J.F. Hainfeld, I. Willner, Science 299 (2003) 1877–1881.
[20] S. Wu, P.P. Liang, H.X. Yu, X.W. Xu, Y. Liu, X.H. Lou, Y. Xiao, Anal. Chem. 86 (2014) 3461–3467.
[21] P. Liu, X.H. Yang, S. Sun, Q. Wang, K.M. Wang, J. Huang, J.B. Liu, L.L. He, Anal. Chem. 85 (2013) 7689–7695.
[22] X.K. Ding, D.D. Ge, K.L. Yang, Sens. Actuators B: Chem. 201 (2014) 234–239.
[23] J.H. Wei, L.T. Zheng, X. Lv, Y.H. Bi, W.W. Chen, W. Zhang, Y. Shi, L. Zhao, X.M. Sun, F. Wang, S.H. Cheng, J.H. Yan, W.J. Liu, X.Y. Jiang, G.F. Gao, X.B. Li, ACS Nano 8 (2014) 4600–4607.
[24] J.J. Du, S.Y. Yin, L. Jiang, B. Ma, X.D. Chen, Chem. Commun. 49 (2013) 4196–4198.
[25] J.J. Du, Q. Shao, S.Y. Yin, L. Jiang, J. Ma, X.D. Chen, Small 8 (2012) 3412–3416.
[26] J.J. Du, B.W. Zhu, X.D. Chen, Small 9 (2013) 4104–4111.
[27] G.H. Chen, W.Y. Chen, Y.C. Yen, C.W. Wang, H.T. Chang, C.F. Chen, Anal. Chem. 86 (2014) 6843–6849.
[28] C. Suksai, T. Tuntulani, Chem. Soc. Rev. 32 (2003) 192–202.
[29] C. Lodeiro, J.L. Capelo, J.C. Mejuto, E. Oliveira, H.M. Santos, B. Pedras, C. Nunez, Chem. Soc. Rev. 39 (2010) 2948–2976.
[30] W.Y. Xie, W.T. Huang, J.R. Zhang, H.Q. Luo, N.B. Li, J. Mater. Chem. 22 (2012) 11479–11482.
[31] N. Kanayama, T. Takarada, M. Maeda, Chem. Commun. 47 (2011) 2077–2079.
[32] X.J. Xue, F. Wang, X.G. Liu, J. Am. Chem. Soc. 130 (2008) 3244–3245.
[33] H. Wang, Y.X. Wang, J.Y. Jin, R.H. Yang, Anal. Chem. 80 (2008) 9021–9028.
[34] Z.H. Qing, X.X. He, K.M. Wang, Z. Zou, X. Yang, J. Huang, G.P. Yan, Anal. Methods 4 (2012) 3320–3325.
[35] D. Li, A. Wieckowska, I. Willner, Angew. Chem. Int. Ed. 47 (2008) 3927–3931.
[36] J.S. Lee, M.S. Han, C.A. Mirkin, Angew. Chem. Int. Ed. 46 (2007) 4093–4096.
[37] J.S. Lee, C.A. Mirkin, Anal. Chem. 80 (2008) 6805–6808.
[38] Y.R. Kim, R.K. Mahajan, J.S. Kim, H. Kim, ACS Appl. Mater. Interfaces 2 (2010) 292–295.
[39] C.J. Yu, W.L. Tseng, Langmuir 24 (2008) 12717–12722.
[40] Y.L. Hung, T.M. Hsiung, Y.Y. Chen, Y.F. Huang, C.C. Huang, J. Phys. Chem. C 114 (2010) 16329–16334.
[41] D.B. Liu, W.S. Qu, W.W. Chen, W. Zhang, Z. Wang, X.Y. Jiang, Anal. Chem. 82 (2010) 9606–9610.
[42] N. Ding, H. Zhao, W.B. Peng, Y.J. He, Y. Zhou, L.F. Yuan, Y.X. Zhang, Colloid Surf. A 395 (2012) 161–167.
[43] C.Y. Lin, C.J. Yu, Y.H. Lin, W.L. Tseng, Anal. Chem. 82 (2010) 6830–6837.
[44] T.T. Lou, Z.P. Chen, Y.Q. Wang, L.X. Chen, ACS Appl. Mater. Interfaces 3 (2011) 1568–1573.
[45] D.Y. Su, X. Yang, Q.D. Xia, F. Chai, C.G. Wang, F.Y. Qu, RSC Adv. 3 (2013) 24618–24624.
[46] X.R. Yang, H.X. Liu, J. Xu, X.M. Tang, H. Huang, D.B. Tian, Nanotechnology 22 (2011) 275503.
[47] Y. Li, P. Wu, H. Xu, Z.P. Zhang, X.H. Zhong, Talanta 84 (2011) 508–512.
[48] Y.J. Ma, L. Jiang, Y.J. Mei, R.B. Song, D.B. Tian, H. Huang, Analyst 138 (2013) 5338–5343.
[49] X.J. Chen, Y.B. Zu, H. Xie, A.M. Kemas, Z.Q. Gao, Analyst 136 (2011) 1690–1696.
[50] G.G. Huang, Y.T. Chen, Y.R. Lin, Anal. Methods 6 (2014) 5690–5696.
[51] S. Anandhakumar, R. Rajaram, J. Mathiyarasu, Analyst 139 (2014) 3356–3359.
[52] T.T. Lou, L. Chen, C.R. Zhang, Q. Kang, H.Y. You, D.Z. Shen, L.X. Chen, Anal. Methods 4 (2012) 488–491.
[53] Y.Y. Xu, L. Deng, H. Wang, X.Y. Ouyang, J. Zheng, J.S. Li, R.H. Yang, Chem. Commun. 47 (2011) 6039–6041.
[54] L. Chen, T.T. Lou, C.W. Yu, Q. Kang, L.X. Chen, Analyst 136 (2011) 4770–4773.
[55] A. Esteban-Gamboa, J. Balzarini, R. Esnouf, E. De Clercq, M.J. Camarasa, M.J. Perez-Perez, J. Med. Chem. 43 (2000) 971–983.
[56] J.S. Nowick, J.S. Chen, G. Noronha, J. Am. Chem. Soc. 115 (1993) 7636–7644.
[57] K.C. Grabar, R.G. Freeman, M.B. Hommer, M.J. Natan, Anal. Chem. 67 (1995) 735–743.
[58] Y. Wu, S. Zhan, L. Xu, W. Shi, T. Xi, X. Zhan, P. Zhou, Chem. Commun. 47 (2011) 6027–6029.
[59] M.Y. Zhu, Y. Wang, Y. Deng, L. Yao, S.B. Adeloju, D.D. Pan, F. Xue, Y.C. Wu, L. Zheng, W. Chen, Biosens. Bioelectron. 61 (2014) 14–20.
[60] Y.Q. He, X.B. Zhang, K. Zeng, S.Q. Zhang, M. Baloda, A.S. Gurung, G.D. Liu, Biosens. Bioelectron. 26 (2011) 4464–4470.
[61] Z.Y. Guo, J. Duan, F. Yang, M. Li, T.T. Hao, S. Wang, D.Y. Wei, Talanta 93 (2012) 49–54.
[62] Q.S. Wei, R. Nagi, K. Sadeghi, S. Feng, E. Yan, S.J. Ki, R. Caire, D. Tseng, A. Ozcan, ACS Nano 8 (2014) 1121–1129.

Biographies

Jianjun Du obtained his Ph.D. from the Dalian University of Technology (China) in 2010. In 2010, he attended the Nanyang Technological University (Singapore) as a postdoctoral fellow. He is currently an associate professor at the State Key Laboratory of Fine Chemicals, Dalian University of Technology. His research is focused on fluorogenic and colorimetric probes based on organic and inorganic materials.

Zhenkuan Wang is a master candidate of State Key Laboratory of Fine Chemicals in Dalian University of Technology, China. His main research interests focus on the AuNPs-based colorimetric detection.

Jiangli Fan received her Ph.D. from the Dalian University of Technology (China) in 2005. In 2010, she attended the University of South Carolina as a visiting scholar. She is currently an associate professor at the State Key Laboratory of Fine Chemicals, Dalian University of Technology. Her research is focused on fluorescent dye-based probes and their biological applications.

Xiaojun Peng received his Ph.D. from the Dalian University of Technology in 1990. After completing a postdoctoral research in Nankai University, he worked at the Dalian University of Technology in 1992. In 2001 and 2002, he attended the Stockholm University and Northwestern University as a visiting scholar. He is currently the professor and director of the State Key Laboratory of Fine Chemicals at the Dalian University of Technology. His research interests cover fluorescent dyes for the bio-imaging, biolabelling, and photochemistry of supramolecules.